Evaluation of Cutting Forces and Prediction of Chatter Vibrations in Milling

H. B. Lacerda and V. T. Lima
Federal University of Uberlândia
School of Mechanical Engineering
Av. João Naves de Ávila, 2121 – Bl. 1M
38400-902 Uberlândia, MG. Brazil
helder@mecanica.ufu.br
vtlima@mecanica.ufu.br

The prediction of chatter vibrations between the cutter and workpiece is important as a guidance to the machine tool user for an optimal selection of depth of cut and spindle rotation, resulting in maximum chip removal rate without this undesirable vibration. This can be done by some approaches. In this work, an analytical method is applied in which the time-varying directional dynamic milling forces coefficients are expanded in Fourier series and integrated in the width of cut bound by entry and exit angles. The forces in the contact zone between cutter and workpiece during the cut are evaluated by an algorithm using a mathematical model derived from several experimental tests with a dynamometer located between the workpiece and machine table. The algorithm results depend of the physical properties of the workpiece material and the cutter geometry. The modal parameters of the machine-workpiece-tool system like natural frequencies, damping and residues must also be identified experimentally. At this point, it is possible to plot the stability lobes to this dynamic system. These curves relates the spindle speed with axial depth of cut, separating stable and unstable areas, allowing the selection of cutting parameters resulting maximum productivity, with acceptable surface roughness and absence of chatter vibrations. Experimental face milling tests were performed in a knee-type machine, using a five inserts cutter. The results showed perfect agreement between chatter prediction and experimental tests.
***Keywords**: Milling, cutting forces, chatter vibrations*

Introduction

The milling operation is a cutting process using a rotating cutter with one or more teeth. An important feature is that the action of each cutting edge is intermittent and cuts less than half of the cutter revolution, producing varying but periodic chip thickness and an impact when the edge touches the workpiece. The tooth is heated and stressed during the cutting part of the cycle, followed by a period when it is unstressed and allowed to cool. The consequences are thermal and mechanical fatigue of the material and vibrations, which are of two kinds: forced vibrations, caused by the periodic cutting forces acting in the machine structure and chatter vibrations, which may be explained by two distinct mechanisms, called "mode coupling" and "regeneration waviness", explained in Tobias (1965), Koenigsberger & Tlusty (1967) and Budak & Altintas (1995). The mode coupling chatter occurs when forced vibrations are present in two directions in the plane of cut. The regenerative chatter is a self-excitation mechanism associated with the phase shift between vibrations waves left on both sides of the chip and happens earlier than the mode coupling chatter in most machining cases, as explained by Altintas (2000). In milling, one of the machine tool-workpiece system structural modes is initially excited by cutting forces. The waved surface left by a previous tooth is removed during the succeeding revolution, which also leaves a wavy surface due to structural vibrations. The cutting forces become oscillatory whose magnitude depends on the instantaneous chip dynamic thickness, which is a function of the phase shift between inner and outer chip surface. The cutting forces can grow until the system becomes unstable and the chatter vibrations increase to a point when the cutter jumps out of the cut or cracks due the excessive forces involved. These vibrations produce poor surface finishing, noise and reduce the life of the cutter. In order to avoid these undesirable effects, the feedrate and the depth of cut are chosen at conservative values, reducing the productivity.

Presented at COBEF 2003 – II Brazilian Manufacturing Congress, 18-21 May 2003, Uberlândia, MG. Brazil.
Paper accepted October, 2003. Technical Editor: Alisson Rocha Machado.

The rotating cutting force, the variable chip thickness and the intermittent cutting periods complicate the use of orthogonal chatter theory to milling operations. Some techniques were developed to select the spindle speed and depth of cut in order to guarantee a system free of chatter vibrations. In this paper, the analytical chatter prediction method presented by Budak & Altintas (1998) was applied to obtain the stability lobes for a vertical milling machine (ROMI™ Interact 4) to predict the occurrence of chatter vibrations. The machining tests showed perfect agreement between prediction and the actual machine behaviour.

Nomenclature

a = *Axial depth of cut, m*
A_0 = *Matrix of average values of* α
F_{rj} = *Radial force, N*
F_{tj} = *Tangential force, N*
$F_{x,y}$ = *Cutting force in direction x or y, N*
$g(\phi_j)$ = *Unit step function, dimensionless*
$H(\phi_j)$ = *Dynamic chip thickness, m*
I = *Identity matrix*
K_r = *Radial cutting constant, dimensionless*
K_t = *Specific cutting energy, N/m²*
n = *Speed spindle, rpm*
N = *Number of teeth of the cutter*
r = *Vibration vector in present period of time (t), m*
r_0 = *Vibration vector in previous period of time (t - T), m*
s_t = *Feed rate per tooth, m/tooth*
T = *Tooth period* ($T = 2\pi/\omega$), *s*
v_j = *Cutter dynamic displacement, m*
x = *Dynamic displacement in feed direction (X), m*
y = *Dynamic displacement in normal direction (Y), m*
ω = *Tooth passing frequency* ($\omega = N.\Omega$), *rad/s*
ω_c = *Chatter frequency, rad/s*

Greek Symbols

α = Directional dynamic milling force coefficient
Δ = Dynamic displacement of the cutter structure, mm
ϕ = Angle of tooth in the cut, deg.

ξ = Damping factor
Ω = Angular speed, rad/s
Φ = Displacement to force transfer function, m/N

Subscripts

c = relative to chatter frequencies
ex = relative to exit angle of tooth in cut
j = relative to tooth number
r = relative to radial direction
st = relative to start angle of tooth in cut
t = relative to tangential direction
x = relative a x direction
y = relative to y direction
0 = relative to a previous rotation, period or tooth

Chatter Vibrations in Milling

The following two sections are indispensable for reader comprehension and were summarised from Altintas (2000). Consider a milling cutter with two degrees of freedom and N number of teeth with a zero helix angle as shown in Figure 1. The cutting forces excite the structure in feed direction X and normal direction Y, causing dynamic displacements x and y, respectively. The dynamic displacements are carried to rotating tooth number j in the radial or chip thickness direction with the following coordinate transformation :

$$v_j = -x \cdot \sin\phi_j - y\cos\phi_j \tag{1}$$

where ϕ_j is the instantaneous angular position of tooth j measured clockwise from the normal Y axis. If the spindle rotates at an angular speed of Ω (rad/s), the angular position varies with time as $\phi_j(t) = \Omega t$, and the cutter pitch angle is $\phi_p = 2\pi/N$.

The resulting chip thickness consists of a static part ($s_t.\sin\phi$) due to the rigid body motion of the cutter and a dynamic component caused by vibrations of the tool at the present and previous tooth periods. The total chip load may be expressed by:

$$h(\phi_j) = [s_t \cdot \sin\phi_j + (v_{j,0} - v_j)] \cdot g(\phi_j) \tag{2}$$

Where s_t is the feed rate per tooth and $v_{j,0}$, v_j are the dynamic displacements of cutter at the previous and present tooth periods. The function $g(\phi_j)$ is a unit step function that indicates if the tooth is in or out of the cut:

$$\begin{aligned} g(\phi_j) &= 1 \longleftarrow \phi_{st} < \varphi_j < \phi_{ex} \\ g(\phi_j) &= 0 \longleftarrow \phi_j < \phi_{st} \quad or \quad \phi_j > \phi_{ex} \end{aligned} \tag{3}$$

The angles ϕ_{st} and ϕ_{ex} represent the start and the exit immersion of the tooth in the cut. The static component of the chip thickness ($s_t.\sin\phi$) is disregarded because it does not contribute to the dynamic chip load regeneration mechanism. So the expression that represents the dynamic displacements of the cutter structure at the present and previous period becomes:

$$h(\phi_j) = [\Delta x \cdot \sin\phi_j + \Delta y \cdot \cos(\phi_j)] \cdot g(\phi_j) \tag{4}$$

where:

$$\Delta x = x - x_0 \quad ; \quad \Delta y = y - y_0 \tag{5}$$

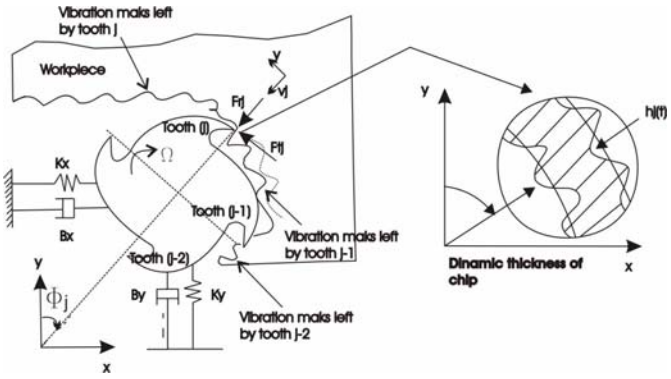

Figure 1. Milling system (2 DOF), with self-excited vibrations. Source: Altintas (2000).

The forces exerted on the tool can now be calculated. The tangential cutting force F_{tj} is assumed to be proportional to the chip thickness and the axial depth of the cut a. The radial force F_{rj} is proportional to F_{tj}.

$$F_{tj} = K_t \cdot a \cdot h(\phi_j); \quad F_{rj} = K_r.F_{tj} \tag{6}$$

where the cutting coefficients K_t and K_r are constants. Solving the cutting forces contributed by all teeth in the x and y directions:

$$\begin{Bmatrix} F_x \\ F_y \end{Bmatrix} = \sum_{j=0}^{N-1} \begin{bmatrix} -\cos\phi_j & -\sin\phi_j \\ \sin\phi_j & -\cos\phi_j \end{bmatrix} \cdot \begin{Bmatrix} F_{tj} \\ F_{rj} \end{Bmatrix} \tag{7}$$

Substituting the chip thickness (Eq. 4) and the tooth forces (Eq. 6) into Eq.(7) and rearranging:

$$\begin{Bmatrix} F_x(t) \\ F_y(t) \end{Bmatrix} = \frac{1}{2} \cdot a \cdot K_t \cdot \begin{bmatrix} \alpha_{xx}(t) & \alpha_{xy}(t) \\ \alpha_{yx}(t) & \alpha_{yy}(t) \end{bmatrix} \cdot \begin{Bmatrix} \Delta x(t) \\ \Delta y(t) \end{Bmatrix} \tag{8}$$

As the cutter rotates, the directional factors α_{ii} vary with time. However, the matrix is periodic at tooth passing frequency ($\omega = N.\Omega$), thus it can be expanded into a Fourier series. In order to simplify the problem, only the average coefficient of the series expansion is considered (r = 0), resulting the components of the directional dynamic milling force coefficients matrix, which are time-invariant but immersion-dependent.

$$\begin{aligned} \alpha_{xx} &= \frac{1}{2} \cdot \left[\cos 2\phi - 2K_r\phi + K_r \sin 2\phi\right]_{\phi_{st}}^{\phi_{ex}} \\ \alpha_{xy} &= \frac{1}{2} \cdot \left[-\sin 2\phi - 2\phi + K_r \cos 2\phi\right]_{\phi_{st}}^{\phi_{ex}} \\ \alpha_{yx} &= \frac{1}{2} \cdot \left[-\sin 2\phi + 2\phi + K_r \cos 2\phi\right]_{\phi_{st}}^{\phi_{ex}} \\ \alpha_{yy} &= \frac{1}{2} \cdot \left[-\cos 2\phi - 2K_r\phi - K_r \sin 2\phi\right]_{\phi_{st}}^{\phi_{ex}} \end{aligned} \tag{9}$$

The dynamic milling forces (Eq. 8) are reduced to the following:

$$\begin{Bmatrix} F_x(t) \\ F_y(t) \end{Bmatrix} = \frac{1}{2} \cdot a \cdot K_t \cdot [A_0] \cdot \begin{Bmatrix} \Delta x(t) \\ \Delta y(t) \end{Bmatrix} \tag{10}$$

Linear Stability Theory

The first step to obtain the stability lobes diagram is to identify experimentally the transfer function matrix which relates the forces and displacements at the cutter-workpiece contact zone:

$$\left[\Phi(iw)\right] = \begin{bmatrix} \Phi_{xx}(iw) & \Phi_{xy}(iw) \\ \Phi_{yx}(iw) & \Phi_{yy}(iw) \end{bmatrix} \tag{11}$$

where $\Phi_{xx}(iw)$ and $\Phi_{yy}(iw)$ are the direct transfer functions in the x and y directions, and $\Phi_{xy}(iw)$ and $\Phi_{yx}(iw)$ are the cross transfer functions. The second step is to calculate the dynamic cutting coefficients from the Eq.(9) for a specified cutter, workpiece material and radial immersion of the cut. Then, a chatter frequency is selected from transfer functions around a dominant mode and the quadratic equation must be solved:

$$a_0 \cdot \lambda^2 + a_1 \cdot \lambda + 1 = 0 \tag{12}$$

where:
$$a_0 = \Phi_{xx}(i\omega_c) \cdot \Phi_{yy}(i\omega_c) \cdot (\alpha_{xx} \cdot \alpha_{yy} - \alpha_{xy}\alpha_{yx})$$
$$a_1 = \alpha_{xx} \cdot \Phi_{xx}(i\omega_c) + \alpha_{yy} \cdot \Phi_{xx}(i\omega_c)$$

The critical depth of cut is evaluated from the real and imaginary part of the eigenvalue $\lambda = \lambda_R + j.\lambda_I$:

$$a_{\lim} = -\frac{2\pi \cdot \lambda_R}{N \cdot K_t} \cdot \left[1 + \left(\frac{\lambda_I}{\lambda_R}\right)^2\right] \tag{13}$$

Now, the spindle speed (rpm) is calculated for each stability lobe from the following equation, where T is the tooth passing period:

$$n = \frac{60}{N \cdot T} \tag{14}$$

Experimental Results

The chatter stability analysis procedure was applied in order to predict the beginning of chatter vibrations in face milling operations performed with a vertical milling machine, using two materials: GH-190 cast iron and ABNT 1020 steel. The experimental tests consist of three parts: 1) identification of the specific cutting energy of the workpiece material and the tool geometric constant; 2) identification of machine tool dynamic parameters; 3) machining tests using depths of cut around the predicted limit.

Part 1. Identification of Specific Cutting Energy (Kt) and Tool Geometric Constant (Kr)

First, the cutting forces during the up and down milling of both materials were measured with a Kistler® dynamometer. Then, the chip medium thickness was evaluated in each test by using the feedrate and spindle speed and Eq.(4). Finally, the specific cutting energy K_t and the tool geometric constant K_r were calculated using Eq.(6) and Eq.(10). Figure 2 shows the experimental apparatus used in this part of the work.

In order to simplify the data analysis and the constants calculation, only one teeth should be cutting at a time. The cutter has 63 mm diameter and five tooth, so the angular spacing is 72 degree and the radial immersion of the cutter into the material should be 21.74 mm. The machining parameters used in the tests are given in the Table 1. A detailed description of this procedure can be found in Lima (2003).

The specific cutting energy (K_t) is not constant during the milling operation and varies with the cutting forces, which are a function of the cutter angular position. The cutter material hardness also influences K_t. However, the error in considering it constant is small when evaluating the chatter stability curves (Smith & Tlusty, 1990). In this work, it is utilised the average value, corresponding to the angular positions where the cutting forces are maximum, in five cutter consecutive rotations. As an illustration, the Fig. 3 shows an example of the measured cutting forces and Table 2 shows K_t and K_r values obtained in the tests.

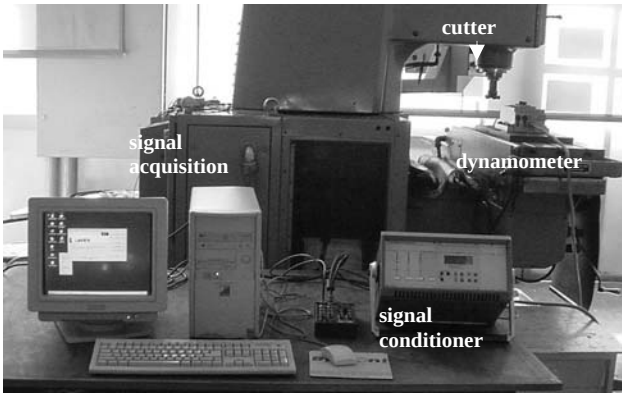

Figure 2. Experimental apparatus for K_r and K_t constants identification.

Table 1. Machining parameters during cutting force acquisition.

Parameters	Up milling	Down milling
Spindle speed (rpm)	1000	1000
Chip load (mm/teeth)	0.05	0.05
Feedrate (mm/min)	250	250
Depth of cut (mm)	0.5 / 1.0 / 1.5	0.5 / 1.0 / 1.5
Start angle (degree)	270	18
Exit angle (degree)	342	90

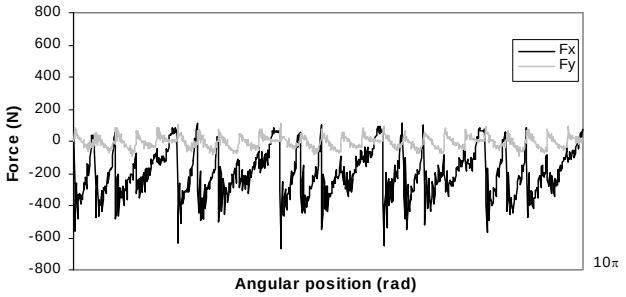

Figure 3. Cutting forces for down milling of cast iron GH 190 during 5 cutter rotations. Depth of cut = 1.0 mm. Spindle speed = 1000 rpm. Feedrate = 250 mm/min.

Table 2 shows that K_t is larger for down milling compared to up milling for both materials. This fact is due to the higher values of the cutting forces in down milling, because of the tool-workpiece impact when the teeth enters in the material. In up milling, the entry of the teeth into the material is mitigated due to the zero initial chip thickness. As a consequence, the stability curves for both materials in down milling predict smaller limit axial depths of cut, when compared with the curves plotted for up milling. Another important observation is that K_t is larger to the GH 190 cast iron due to its higher hardness. This fact results in smaller limit axial depths of cut for this material when compared with ABNT 1020 steel.

Table 2. Variation of K_t and K_r with depth of cut in DOWN and UP milling of cast iron GH 190 and ABNT 1020 steel.

	Material		Depth of cut (mm)			Average
			0.5	1.0	1.5	
DOWN	GH 190	K_t (Mpa)	4337	3789	4077	**4068**
		K_r (ad.)	0.53	0.53	0.54	**0.53**
	ABNT 1020	K_t (Mpa)	3579	3305	3410	**3431**
		K_r (ad.)	0.54	0.53	0.52	**0.53**
UP	GH 190	K_t (Mpa)	2421	2547	2505	**2491**
		K_r (ad.)	1.14	1.08	1.11	**1.11**
	ABNT 1020	K_t (Mpa)	2379	2105	2119	**2201**
		K_r (ad.)	1.07	1.14	1.09	**1.10**

Part 2. Identification of System Dynamic Parameters

In order to evaluate the chatter stability curves, it is necessary to identify modal parameters of the machine-workpiece-cutter dynamic system. The transfer functions which relate the displacements with the forces applied in directions X and Y must be obtained, and also the residues. The table position, the cutter size and its vertical position influences the machine natural frequencies. The table was positioned in the centre of the work area and the cutter vertical position, 50 mm bellow the highest position. The cutter has double positive geometry, five teeth and 63 mm diameter and can be seen in Fig. 4b.

The machine structure was excited in two different points (Fig. 4a) with a impact hammer instrumented with a piezoelectric force transducer. These points are the spindle inferior bearing and the cutter edge. The impact force has a short duration and can be considered as a pulse (see Fig. 4c). The plastic tip was chosen to excite preferably the low and medium natural frequencies. The accelerometer was also positioned in both points alternately. The accelerometer signal conditioner was regulated to measure the displacements (Fig. 4d) at these points, which were chosen based on the sensibility studies of Souza (1998), who pointed them as the better ones to measure the signals at this machine. Ten impacts were produced in each of the four tests (to have an average) and the signals from the force transducer and the accelerometer were acquired by using a data acquisition system.

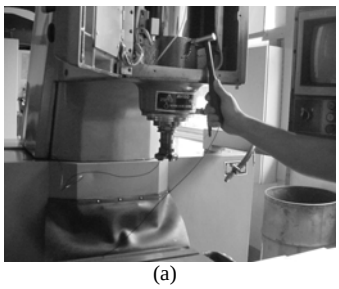

(a)

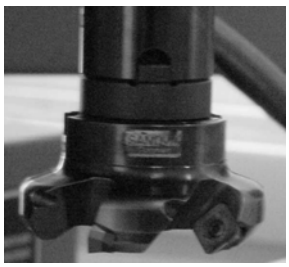

(b)

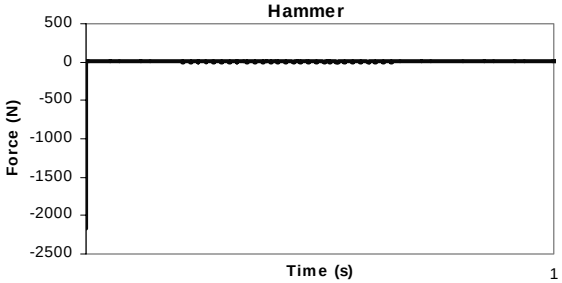

(c)

Figure 4. Experimental parameters identification. (a) impact in the bearing and accelerometer attached on the cutter; (b) cutter; (c) input: impact force; (d) output: cutter displacement.

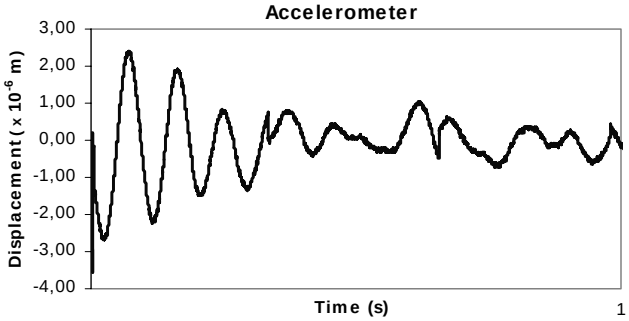

(d)

Figure 4. (Continued).

The Matlab® Identification Toolbox was used to get the transfer functions of the system, which also provided the natural frequencies, damping and residues. The results are given in Table 3:

Table 3. Identified modal parameters.

Mode	ω_n (rad/s)	ξ_n	Residues (m/N)
1	1822	0.1420	-2.8526E-13 – 1.8809E-12i
2	1976	0.0454	-8.8800E-13 – 2.1866E-14i
3	2856	0.0468	2.2093E-13 – 6.9740E-13i
4	3721	0.0980	-2.3216E-13 + 2.3364E-13i

Part 3. Chatter Prediction Curves: Construction and Validation

The stability curves relate the spindle speed with the maximum depth of cut which can be used without chatter vibrations. Then, the chip removal rate can be maximised without possible damages caused by excessive vibration. Each stability curve is valid for a specific kind of milling (up or down), workpiece material (ABNT 1020 steel or GH 190 cast iron) and cutter. The curves were plotted by an algorithm written with Matlab® software, fed with the previously obtained experimental data. The area bellow the curves represents the stability region for the system, free of chatter vibrations. The area above the curve represents the unstable region where chatter vibrations occur. The curves validation is done with experimental vibration tests where the depth of cut and spindle speed combinations were selected by points bellow and above the stability curves. The vibration level was measured by an accelerometer positioned in the inferior spindle bearing. The chatter vibrations produce characteristic sound and superficial marks. These marks can be observed by visual inspection of the workpiece after the test. Due space limitation, only two tests results are going to be shown here: the up milling of ABNT 1020 steel and down milling of GH 190 cast iron.

a) ABNT 1020 Steel Up Milling

The stability curve for up milling of ABNT 1020 steel is shown in Fig. 5. The ten points represent the tests performed with several spindle speed and depth of cut combinations. The feedrate is the same in all tests.

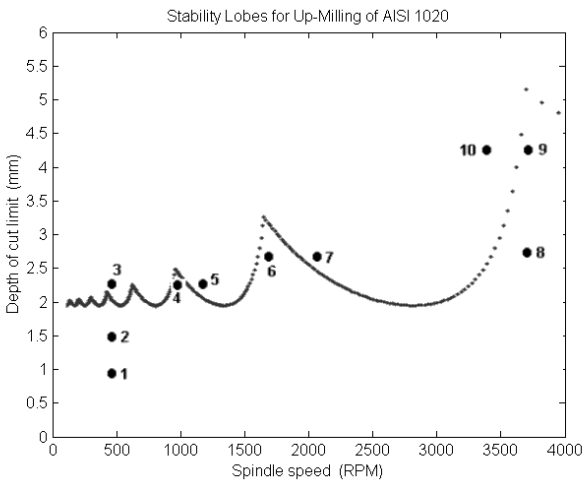

Figure 5. Stability curve for ABNT 1020 steel up milling with the five teeth cutter in Fig. 4b. Feedrate = 0,25 mm / revolution.

The graphs in Fig. 6 and 7 show the displacement vibration signal obtained for test points 2 and 3 marked in Fig. 5. The points 1 and 2 have a small vibration level, because they are in the stable region. The test point 3 is in the graph unstable region and the vibration level resulted four times greater, with the chatter vibration characteristic sound and superficial marks, as predicted by the stability curve.

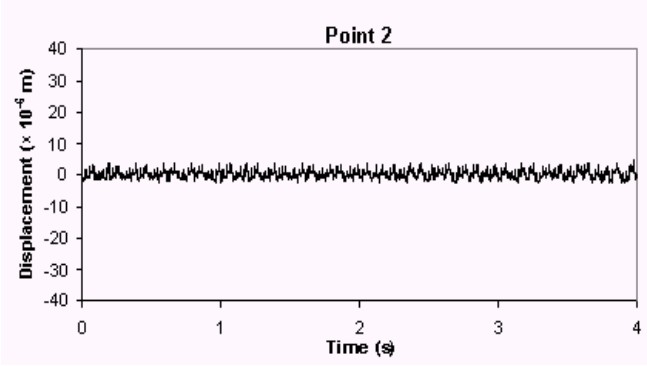

Figure 6. Test point 2 displacement signal.

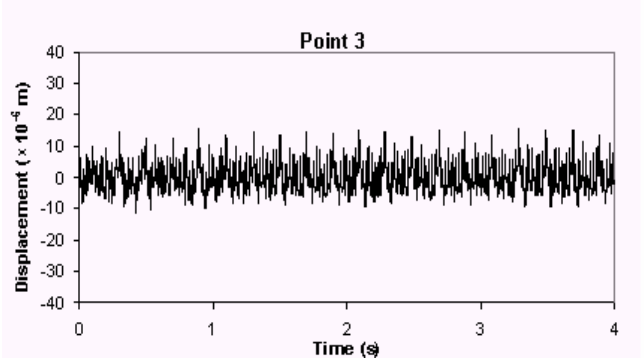

Figure 7. Test point 3 displacement signal.

Figures 8 and 9 show the displacement signal obtained in the test points 4 and 5 (Fig. 5). The depth of cut is the same and point 4 is in stable region, presenting a smaller vibration level than that of points 3 and 5, as expected. The test point 5 showed light chatter vibrations, as predicted by the stability curve.

Figures 10 and 11 present the test points 6 and 7 displacement signal. The depth of cut is the same in both tests. The test point 6 presented a small vibration level and test point 7 resulted severe chatter vibrations, as predicted by the stability curve in Fig. 5. It is interesting to note that test point 6 has a reduced vibrations level when compared with test point 5, in spite of the higher depth of cut and spindle rotation.

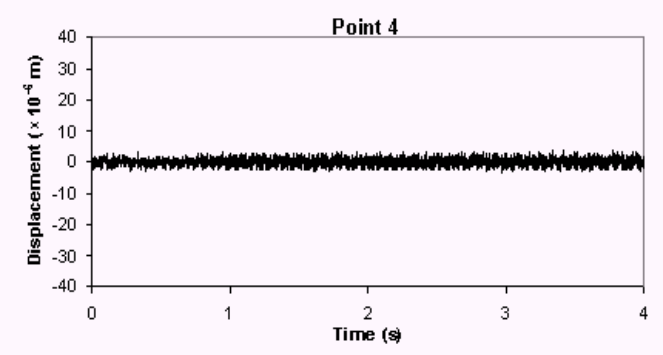

Figure 8. Test point 4 displacement signal.

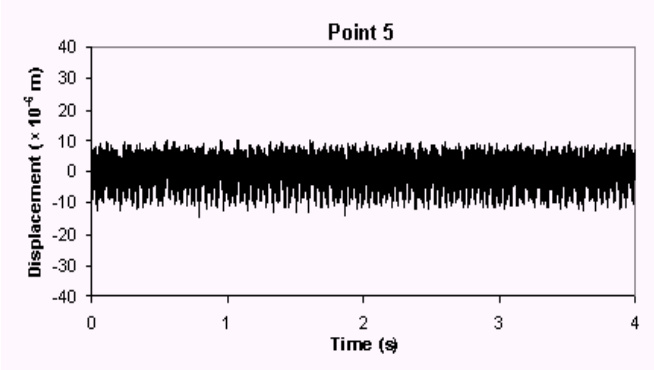

Figure 9. Test point 5 displacement signal.

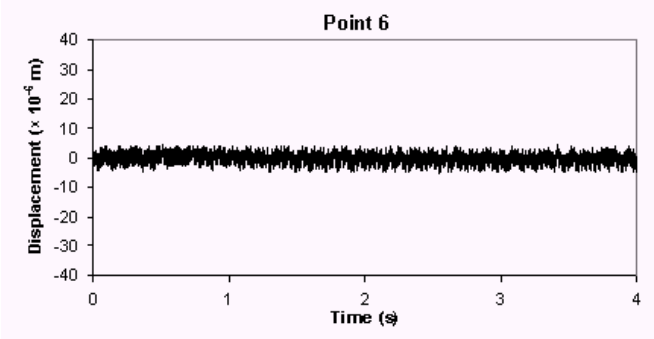

Figure 10. Test point 6 displacement signal.

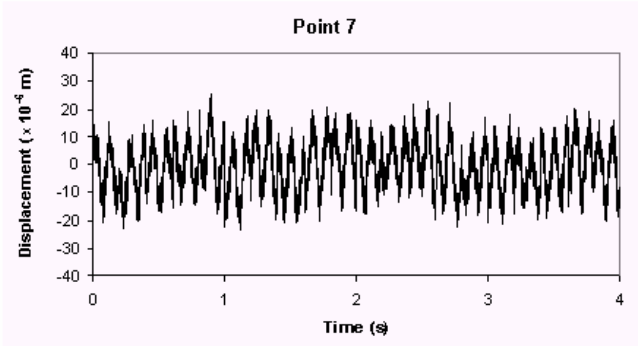

Figure 11. Test point 7 displacement signal.

The test points 8 and 9 are in the stability curve stable region (Fig. 5) and the time domain vibration signals have low amplitude, as can be seen in the Fig. 12 and 13. The point 10 prediction is "chatter", because it is in the unstable region. This was confirmed in the test, with the characteristic sound and marks of chatter vibrations and the five times higher amplitude level signal shown in Fig. 14. For a better comparison, the RMS of all the test points vibration signals is shown in the Fig. 15.

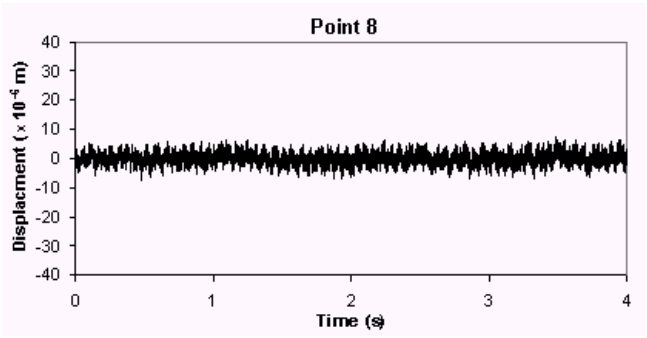

Figure 12. Test point 8 displacement signal.

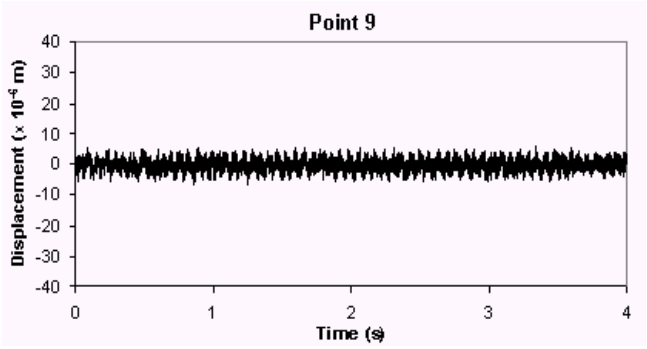

Figure 13. Test point 9 displacement signal.

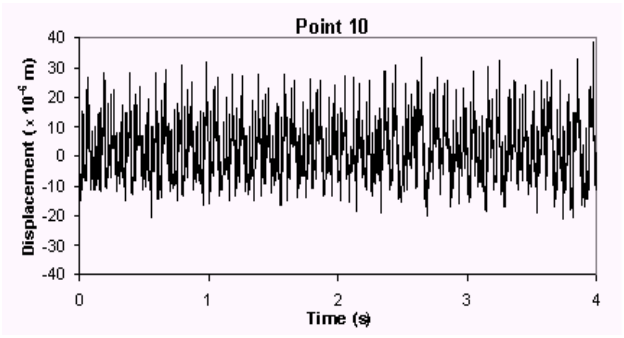

Figure 14. Test point 10 displacement signal.

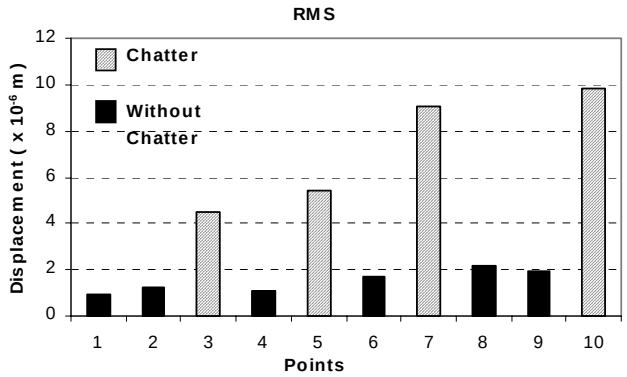

Figure 15. Stability curve test points RMS levels, for ABNT 1020 steel up milling.

b) GH 190 Cast Iron Down Milling

The stability curve for GH 190 cast iron down milling is shown in Fig. 16. The ten points represent the down milling tests performed with several spindle speed and depth of cut combinations. The feedrate is the same in all tests. The curve format is similar, because the cutter and machine modal parameters are unchanged. The depths of cut are smaller to the GH 190 cast iron because the cutting forces and specific cutting energy (K_t) are greater, due to its higher hardness. For both materials, the highest chatter vibration free depth of cut are in the spindle speed range between 3600 and 4000 rpm.

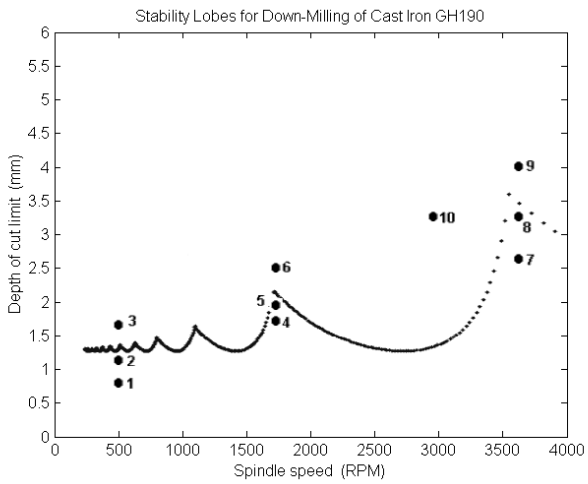

Figure 16. GH 190 cast iron down milling stability curve with the same five teeth cutter in Fig. 4b. Feedrate = 0,25 mm / revolution.

Figures 17 and 18 show the test points 2 and 3 (Fig. 16) displacement vibration signal. The points 1 and 2 have a small vibration level, because they are in the stable region. The test point 3 is in the graph unstable region and the vibration level resulted four times greater, with the chatter vibrations characteristic sound and superficial marks, as predicted by the stability curve.

Figures 19 and 20 show the test points 5 and 6 (Fig. 16) displacement vibration signal. The points 4 and 5 are in the stable region, presenting a small vibration level. The test point 6 showed chatter vibrations, as predicted by the stability curve.

Figures 21 and 22 present the displacement signal measured at test points 7 and 8. They are in the stable region and the vibration level resulted small, as predicted. Figure 23 presents the displacement signal at test point 9, which resulted severe chatter vibrations, as expected. It is interesting to note that test point 8 has a reduced level of vibrations when compared with test point 6, in spite of the higher depth of cut and spindle rotation.

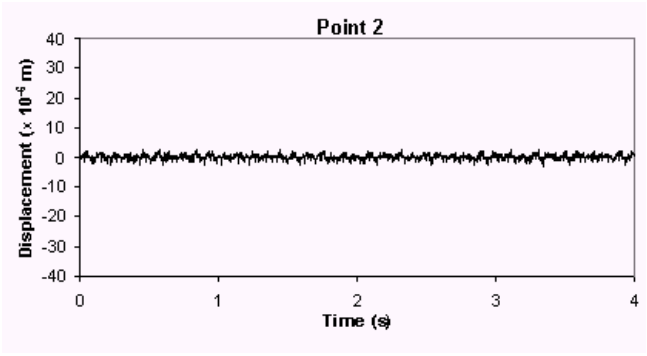

Figure 17. Test point 2 displacement signal.

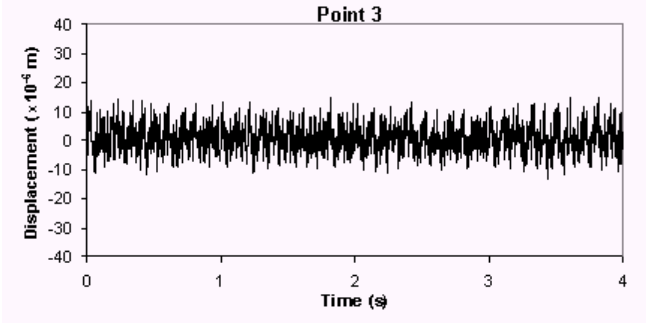

Figure 18. Test point 3 displacement signal.

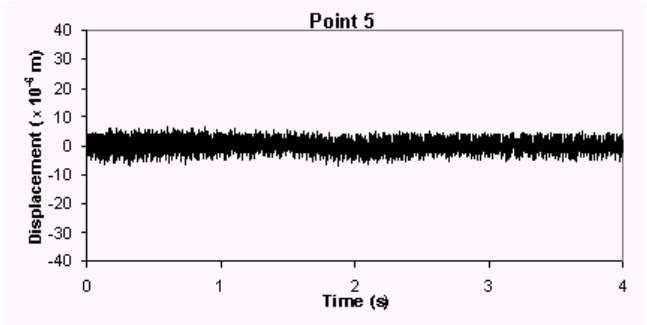

Figure 19. Test point 5 displacement signal.

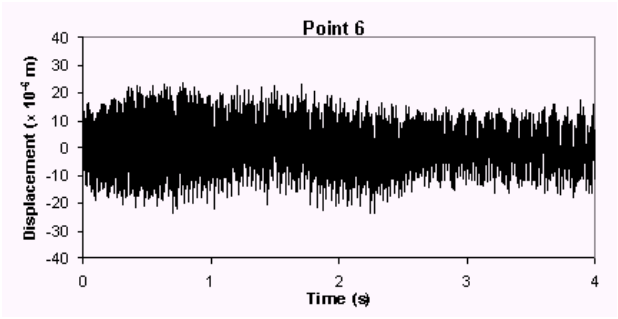

Figure 20. Test point 6 displacement signal.

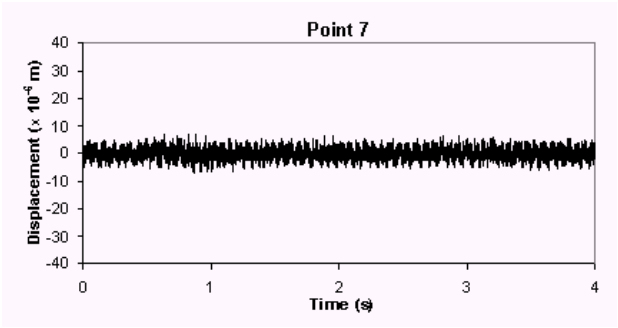

Figure 21. Test point 7 displacement signal.

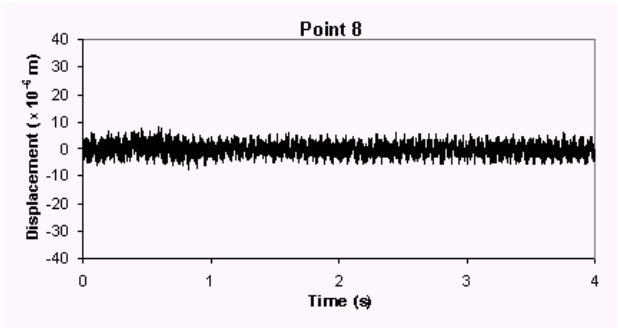

Figure 22. Test point 8 displacement signal.

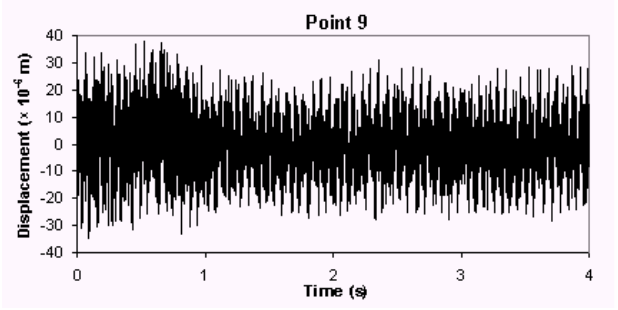

Figure 23. Test point 9 displacement signal.

Figure 24 presents the test point 10 displacement signal located in the graph unstable region in Fig. 16. It was marked by chatter vibrations, as expected. It is interesting to note that test point 8 (in the stable region) has the same depth of cut and higher spindle speed, but only small structural vibrations were observed, again validating the stability curve in Fig. 16. For a better comparison between the tests, the RMS levels are shown in the Fig. 25.

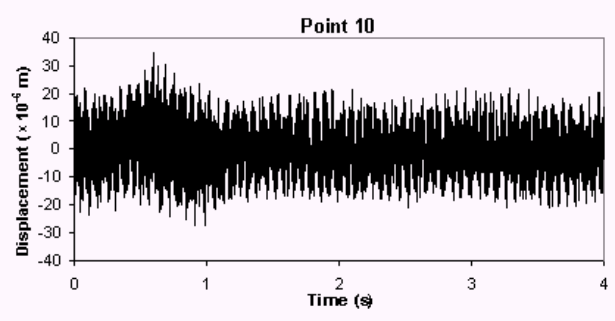

Figure 24. Test point 10 displacement signal.

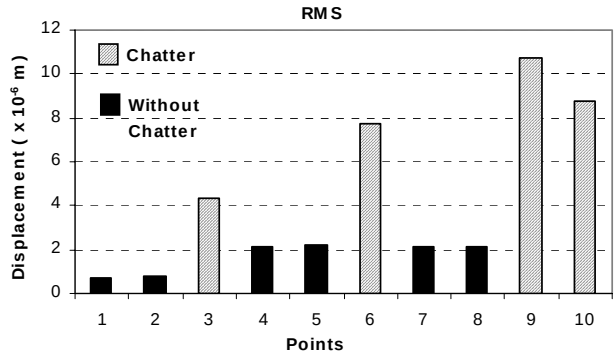

Figure 25. Stability curve test points RMS levels, for GH 190 cast iron down milling.

Conclusions

The main advantage of the chatter prediction through the stability lobes diagram is the metal removal rate maximisation, at the same time avoiding the adverse effects of chatter vibrations like the poor surface finish, noise and breakage of tools.

The analytical method presented by Budak & Altintas (1998) was applied in order to predict the occurrence of chatter vibrations for a vertical milling machine. The method is not simple and its practical implementation depends on experimental tests which require the use of expensive equipment, rarely available at industrial environment. The K_t and K_r constants are evaluated for the specific material-cutter combination, after measuring the cutting forces as explained earlier. The machine modal parameters are influenced by table position, spindle vertical position and the cutter-workpiece-jigs mass. So, one stability curve is valid only for a specific combination of the machine-workpiece-cutter system.

The method is hard to be implemented, but machining tests showed perfect agreement between the prediction and actual machine tool behaviour. Another good characteristic is the elimination of the extremely long time for computational calculation, when applying numerical solution methods.

The depth of cut is the main parameter relative to chatter vibrations: selecting a spindle speed and increasing the depth of cut, a limit is found when these vibrations start with the characteristic sound and workpiece surface marks. The feedrate modifies only the chip thickness static component, which is removed from the equations, because it does not contribute to the dynamic chip load regeneration mechanism, origin of chatter vibrations.

The workpiece material specific cutting energy raises or pull down the stability curves. The greater the K_t value, smaller the limit depth of cut for a stable machine operation. The GH 190 cast iron has a greater K_t, as a consequence of its higher hardness, resulting in smaller depths of cut when compared to the ABNT 1020 steel. The specific cutting energy is influenced by the milling operation type. Down milling presents higher K_t values for both materials, pulling down the stability curves, which results in smaller limit depths of cut when compared to up milling. This fact is a consequence of the higher cutting forces observed in down milling operations, due to teeth-workpiece impact in the start angle.

References

Altintas, Y., 2000, "Manufacturing Automation: Metal Cutting Mechanics, Machine Tool Vibrations, and CNC Design", 1st ed., Ed. Cambridge University Press, NY, USA.

Altintas, Y. and P. Lee, 1996, "A General Mechanics and Dynamics Model for Helical End Mills, Annals of the CIRP, v. 45/1.

Budak, E. and Y. Altintas, 1995, "Analytical Prediction of Stability Lobes in Milling", Annals of CIRP, v. 44 / 1.

Budak, E. et al., 1996, "Prediction of Milling Force Coefficients From Orthogonal Cutting Data", Transactions of the ASME, v. 118.

Budak, E. and Y. Altintas, 1998, "Analytical Prediction of Chatter Stability in Milling, Part I: General Formulation", ASME Journal of Dynamics Systems, Measurements, and Control, v. 120.

Budak, E. and Y. Altintas, 1998, "Analytical Prediction of Chatter Stability in Milling, Part II: Application of General Formulation to Common Milling Systems", ASME Journal of Dynamics Systems, Meas., and Control, v. 120.

Koenigsberger, F. and J. Tlusty, 1967, "Machine Tool Structures – Vol. I: Stability Against Chatter", Pergamon Press.

Lima, V.T., 2003, "Análise e Predição de Vibrações tipo *Chatter* em Operações de Fresamento", Master Thesis, Federal University of Uberlandia – Mechanical Engineering School, Uberlandia, MG, Brazil. 132 p. In Portuguese.

Minis, I. and R. Yanushevsky, 1993, "A New Theoretical Approach for the Prediction of Machine Tool Chatter in Milling", Journal of Engineering for Industry, v. 115.

Smith, S. and J. Tlusty, 1990, "Update on High Speed Dynamics", Transactions of the ASME, v. 112.

Souza, M. M. de, 1998, "Utilizando a Vibração Mecânica para Monitorar o Desgaste das Ferramentas de Corte e Acabamento Superficial no Processo de Fresamento Ph.D. Thesis, Federal University of Uberlandia – Mechanical Engineering School, Uberlandia, MG, Brazil. 101 p. In Portuguese.

Tlusty, J. and F. Ismail, 1981, "Basic Nonlinearity in Machining Chatter", Annals of the CIRP, v. 30, pp. 21-25.

Tobias, S. A., 1965, "Machine Tool Vibrations", Blackie and Sons Ltd.